J|A|C|S ARTICLES

Published on Web 12/13/2010

Lanthanide Clusters with Chalcogen Encapsulated Ln: NIR Emission from Nanoscale $NdSe_x$

Brian F. Moore,[†] G. Ajith Kumar,[‡] Mei-Chee Tan,[‡] Jesse Kohl,[‡] Richard E. Riman,[‡] Mikhail G. Brik,[§] Thomas J. Emge,[†] and John G. Brennan*,[†]

Department of Chemistry and Chemical Biology, Rutgers, The State University of New Jersey, 610 Taylor Road, Piscataway New Jersey 08854-8087, United States, Department of Materials Science and Engineering, Rutgers, The State University of New Jersey, 607 Taylor Road, Piscataway New Jersey 08854-8087, United States, and Institute of Physics, University of Tartu, Riia 142, Tartu 51014, Estonia

Received August 13, 2010; E-mail: bren@rci.rutgers.edu

Abstract: $Ln(SePh)_3$ (Ln = Ce, Pr, Nd) reacts with elemental Se in the presence of Na ions to give $(py)_{16}Ln_{17}NaSe_{18}(SePh)_{16}$, a spherical cluster with a 1 nm diameter. All three rare-earth metals form isostructural products. The molecular structure contains a central Ln ion surrounded by eight five-coordinate Se^{2-} that are then surrounded by a group of 16 Ln that define the cluster surface, with additional μ_3 and μ_5 Se^{2-}, μ_3 and μ_4 $SePh^-$, and pyridine donors saturating the vacant coordination sites of the surface Ln, and a Na ion coordinating to selenolates, a selenido, and pyridine ligands. NIR emission studies of the Nd compound reveal that this material has a 35% quantum efficiency, with four transitions from the excited state $^4F_{3/2}$ ion to $^4I_{9/2}$, $^4I_{11/2}$, $^4I_{13/2}$, and $^4I_{15/2}$ states clearly evident. The presence of Na^+ is key to the formation of these larger clusters, where reactions using identical concentrations of $Nd(SePh)_3$ and Se with either Li or K led only to the isolation of $(py)_8Nd_8Se_6(SePh)_{12}$.

Introduction

Control of near-infrared (NIR) emission from lanthanide ions is a fundamentally important topic that is key to the continued development of next generation optical fiber technologies.[1] The most extensively used optical materials today are oxide glasses that depend entirely on 1.54 μm emission from Er(III) ions because this lanthanide is the only emission source that emits within the oxide transmission window.[2] The development of alternative fiber materials with broader transmission windows, that is, those based on organic polymers,[3] is an active field of research. Functional polymer fibers are hampered by the difficulty of incorporating emissive Ln ions into an apolar polymer matrix.

Molecular sources of NIR emissive lanthanides are obvious candidates for incorporation into polymers, but in molecular systems, emissions are not bright enough for many applications because Ln excited states are not easily populated, and ligands have vibrational modes that quench emission. Ligands have been synthetically modified to eliminate functional groups with high energy stretching frequencies that are particularly detrimental to NIR emission, that is, replacement of C−H with C−D[4] or C−F[5] has been shown to significantly improve properties in a series of Nd compounds, while replacement of Ln−O[6] with Ln−S[7] has generated the most efficient molecular NIR sources to date.

Even with these improvements, the utility of molecular NIR sources is limited by the fact that molecular coordination spheres occupy a significant volume, and this 'wasted space' precludes the synthesis of materials with significant concentrations of

[†] Department of Chemistry and Chemical Biology, Rutgers.
[‡] Department of Materials Science and Engineering, Rutgers.
[§] University of Tartu.

(1) Kuriki, K.; Koiki, Y.; Okamoto, Y. *Chem. Rev.* **2002**, *102*, 2347.
(2) Becker, P. C.; Olsson, N. A.; Simpson, J. R. *Erbium Doped Fiber Amplifiers—Fundamentals and Technology*; Academic Press: San Diego, CA, 1999.
(3) (a) Kuriki, K.; Kobayashi, T.; Imai, N.; Tamura, T.; Nishihara, S.; Tagaya, A.; Koike, Y.; Okamoto, Y. *IEEE Photonics Technol. Lett.* **2000**, *12*, 989. (b) Xu, X. *Opt. Commun.* **2003**, *225*, 55. (c) Zheng, Z.; Liang, H.; Ming, H.; Zhang, Q.; Xie, J. *Opt. Commun.* **2004**, *233*, 149. (d) Liang, H.; Zheng, Z.; Chen, B.; Zhang, Q.; Ming, H. *Mater. Chem. Phys.* **2004**, *86*, 430. (e) Kuriki, K.; Nishihara, S.; Nisizawa, Y.; Yosinaga, T.; Tagaya, A.; Koike, Y.; Okamoto, Y. *Opt. Lett.* **2003**, *28*, 570. (f) Liang, H.; Zhang, Q.; Zheng, Z.; Ming, H.; Li, Z.; Xu, J.; Chen, B.; Zhao, H. *Opt. Lett.* **2004**, *29*, 477.
(4) (a) Hebbink, G. A.; Reinhoudt, D. N.; van Veggel, F. C. J. M. *Eur. J. Org. Chem.* **2001**, 4101. (b) Hasegawa, Y.; Ohkubo, T.; Sogabe, K.; Kawamura, Y.; Wada, Y.; Nakashima, N.; Yanagida, S. *Angew. Chem.* **2000**, *112*, 365. (c) Van Deun, R.; Nockemann, P.; Görller-Walrand, C.; Binnemans, K. *Chem. Phys. Lett.* **2004**, *397*, 447.
(5) (a) Rusakova, N. V.; Topilova, Z. M.; Meshkova, S. B.; Lozinskii, M. O.; Gevaza, Y. I. *Russ. J. Inorg. Chem.* **1992**, *37*, 116. (b) Hasegawa, Y.; Murakoshi, K.; Wada, Y.; Yanagida, S.; Kim, J.-H.; Nakashima, N.; Yamanaka, C. *Chem. Phys. Lett.* **1996**, *248*, 8. (c) Batista, H. J.; De Andrade, A.; Longo, R. L.; Simas, A. M.; De Sa, G. F.; Ito, K. N.; Thompson, L. C. *Inorg. Chem.* **1998**, *37*, 3542. (d) Chauvin, A.; Gumy, F.; Matsubayashi, I.; Hasegawa, Y.; Bünzli, J. C. G. *Eur. J. Inorg. Chem.* **2006**, 473. (e) Glover, P. B.; Bassett, A. P.; Nockemann, P.; Kariuki, B. M.; Van Deun, R.; Pikramenou, Z. *Chem.—Eur. J.* **2007**, *13*, 6308.
(6) Norton, K.; Kumar, G. A.; Dilks, J. L.; Emge, T. J.; Riman, R. E.; Brik, M. G.; Brennan, J. G. *Inorg. Chem.* **2009**, *48*, 3573.
(7) (a) Banerjee, S.; Kumar, G. A.; Emge, T. J.; Riman, R. E.; Brennan, J. G. *Chem. Mater.* **2008**, *20*, 4367. (b) Kumar, G. A.; Kornienko, A.; Banerjee, S.; Riman, R. E.; Emge, T. J.; Brennan, J. G. *Chem. Mater.* **2005**, *17*, 5130. (c) Banerjee, S.; Huebner, L.; Romanelli, M. D.; Kumar, G. A.; Riman, R. E.; Emge, T. J.; Brennan, J. G. *J. Am. Chem. Soc.* **2005**, *127*, 15900. (d) Riman, R.; Kumar, G. A.; Bannerjee, S.; Brennan, J. G. *J. Am. Ceram. Soc.* **2006**, *89*, 1809.

emissive Ln. For example, $(DME)_2Ln(SC_6F_5)_3$ are currently the most emissive molecules in the literature, but the preparation of functional waveguides with this compound serving as the signal amplifier would require a 1:10 $Ln(SC_6F_5)_3$/polymer ratio.[8] Thiolate concentrations at this level would have a deleterious impact on the transmission properties (i.e., changing refractive index) of any host polymer.

Cluster compounds have an intrinsically large concentration of metal ions; compare, for example, the [Er] in the crystal structures of molecular $(DME)_2Er(SC_6F_5)_3$ (1.2×10^{21} ions/cc) with the nanoscale cluster $(THF)_{10}ErS_6(SeSe)_6I_6$ (3.4×10^{21} ions/cc). With these higher Ln concentrations, clusters become comparable to rare earth doped ceramic hosts[7d] and are an attractive alternative to conventional molecular Ln polymer amplifiers. In addition, the precise manner in which single crystal X-ray diffraction can define a cluster structure allows us to develop a fundamental understanding of how cluster structure impacts on NIR emission properties.[7c,9−12] This knowledge could be pivotal to the successful design and fabrication of organic waveguides. A variety of anions have been used to assemble multimetallic species, and it appears from this work that emission properties depend significantly on the identity and phonon environment generated by the anion. Unfortunately, there are no similarly sized clusters constructed from different anions, and so there is no way to evaluate how the cluster anions influence quantum efficiency. Materials with similar sizes would be helpful because some intensity is unavoidably lost to vibrational modes of the ligands on the cluster surface (i.e., C−H vibrations in THF, SeC_6H_5), and similar [Ln]/[C−H] ratios for different cluster types would provide an opportunity to examine how anion identity influences emission properties. To date, larger chalcogenido clusters with both internal and surface Ln were known only for the later lanthanides (Dy, Ho, Er),[9] while fluoride clusters with internal and surface Ln were known only for the early lanthanides (Pr, Nd).[11]

In the process of looking at methods to control the surface chemistry of cluster compounds, we found that when $Ln(SePh)_3$ (Ln = Ce, Pr, Nd) react with elemental Se in the presence of Na^+, heptadecanuclear selenido clusters can be isolated in high yield. We describe here the synthesis and structure of these products, and a detailed analysis of the emission properties of the Nd compound. These compounds permit a more direct evaluation of how anions impact quantum efficiency in nanoscale clusters.

Experimental Section

General Methods. All syntheses were carried out under ultra pure nitrogen (Welco Praxair), using conventional drybox or Schlenk techniques. Pyridine (Aldrich) was purified with a dual column Solv-Tek solvent purification system and collected immediately prior to use. PhSeSePh was purchased and recrystallized from hexane. Nd (Strem) and Hg (Aldrich) metals were purchased and used as received. Melting points were recorded in sealed capillaries and are uncorrected. FTIR spectra were recorded on a Thermo Nicolet Avatar 360 FTIR spectrometer from 4000 to 450 cm^{-1} as Nujol mulls on CsI plates. Elemental analyses were performed by Quantitative Technologies, Inc. (Whitehouse, NJ). In addition to air sensitivity, these compounds are thermally unstable and tend to lose lattice pyridine within minutes of isolation. Calculated elemental analyses values are given for the cluster and for the cluster with lattice solvent in parentheses.

Synthesis of $(py)_{16}Ce_{17}Se_{18}(SePh)_{16}Na$ (1). Ce (937 mg, 6.68 mmol), PhSeSePh (960 mg, 3.07 mmol), and Hg (23 mg, 0.11 mmol) (added to increase the rate of the reaction) were combined in pyridine (40 mL), and the mixture was stirred for 24 h to give a clear dark yellow solution with some visible metal (solution 1). In a separate Schlenk flask, Na (68.9 mg, 2.99 mmol) and PhSeSePh (468 mg, 1.50 mmol) were combined in pyridine (30 mL) and allowed to stir for 24 h to give a clear yellow solution (solution 2). Selenium (490 mg, 6.20 mmol) was added to solution 1 and stirred for 1 min, and then solution 2 was added to solution 1 and the mixture was stirred for 3 days. The mixture was filtered, concentrated to 20 mL, and layered with hexanes (4 mL) to give reddish orange crystals (2.33 g, 81%) of **1** that turn brown at 220 °C, and melt between 290 and 295 °C. Anal. Calcd for $C_{176}H_{160}N_{16}Se_{34}NaCe_{17}$: C, 25.9(30.4); H, 1.96(2.37); N, 2.57(3.94); Na, 0.24(0.26). Found: C, 26.2; H, 1.46; N, 3.37; Na, 0.26. UV−vis: $\lambda_{max} = 442$ nm ($\varepsilon = 250\ M^{-1}\ cm^{-1}$). IR: 2853 (s), 2726 (w), 2359 (m), 2341(m), 2051(w), 1594 (w),1574 (w), 1462 (s), 1377(s), 1260 (m), 1217 (w), 1146 (w), 1065 (w), 1020 (w), 800 (m), 731 (m), 700 (m) cm^{-1}.

Synthesis of $(py)_{16}Pr_{17}Se_{18}(SePh)_{16}Na$ (2). Pr (940 mg, 6.70 mmol), PhSeSePh (960 mg, 3.07 mmol), and Hg (45 mg, 0.22 mmol) were combined in pyridine (45 mL), and were allowed to stir for 24 h to give a dark yellow clear solution with some visible metal (solution 1). In a separate Schlenk flask, Na (69 mg, 3.00 mmol) and PhSeSePh, (468 mg, 1.50 mmol) were combined in pyridine (30 mL) and allowed to stir for 24 h to give a clear yellow solution with no visible metal (solution 2). Selenium (470 mg, 5.95 mmol) was added to the solution and the mixture was stirred for 1 min. Solution 2 was then added to solution 1 and this mixture was stirred for 3 days. The solution was filtered, concentrated to 20 mL, and layered with hexanes (4 mL) to give yellow green crystals (2.02 g, 93%) that turn brown at 200 °C, and melt between 216 and 220 °C. Anal. Calcd for $C_{176}H_{160}N_{16}Se_{34}NaPr_{17}$: C, 25.9(30.4); H, 1.96(2.36); N, 2.57(3.94); Na, 0.24(0.26). Found: C, 26.9; H, 2.31; N, 2.69; Na, 0.37. UV−vis: $\lambda_{max} = 600$ ($\varepsilon = 6.7\ M^{-1}\ cm^{-1}$), 496, 455 nm. IR: 2922 (s), 2720 (w), 2666 (w), 2059 (w), 1908 (w), 1594 (m), 1573 (m), 1462 (s), 1376 (s), 1298 (m), 1259 (m), 1217 (m), 1147 (m), 1069 (m), 1015 (m), 936 (w), 888 (w), 803 (m), 731 (s), 689 (m) cm^{-1}. Unit cell data (Mo Kα, 100K): $a =$ 22.60(2) Å, $b = 42.11(3)$ Å, $c = 31.10(2)$ Å, $\beta = 108.58(5)°$, $V =$ 28059(46) $Å^3$.

Synthesis of $(py)_{16}Nd_{17}Se_{18}(SePh)_{16}Na$ (3). Nd (960 mg, 6.65 mmol), PhSeSePh (963 mg, 3.08 mmol), and Hg (30 mg, 0.15 mmol) were combined in pyridine (40 mL), and the mixture was allowed to stir for 24 h to give a dark green clear solution with some visible metal (solution 1). In a separate Schlenk flask, Na (69 mg, 3.00 mmol) and PhSeSePh, (468 mg, 1.50 mmol) were combined in pyridine (30 mL) and allowed to stir for 24 h to give a clear yellow solution with no visible metal (solution 2). Selenium (450 mg, 5.69 mmol) was added to solution 1 and the mixture was stirred for 5 min. Solution 2 was then added to solution 1 and this was stirred for 3 days. The combined solution was filtered, concentrated to 20 mL, and layered with hexanes (4 mL) to give light green crystals (2.03 g, 76%) that turn brown between 216 and 219 °C, and do not melt. Anal. Calcd for $C_{176}H_{160}N_{16}Se_{34}NaNd_{17}$: C, 25.7(30.2); H, 1.95(2.35); N, 2.55(3.92); Na, 0.24(0.26). Found: C, 29.9; H, 1.97; N, 3.67; Na, 0.15. IR: 2954 (s), 2925 (s),

(8) (a) Kumar, G. A.; Riman, R. E.; Chen, S.; Smith, D.; Ballato, J.; Banerjee, S.; Kornienko, A.; Brennan, J. G. *Appl. Phys. Lett.* **2006**, *88*, 91902. (b) Kumar, G. A.; Riman, R. E.; Diaz Torres, L. A.; Banerjee, S.; Romanelli, M. D.; Emge, T. J.; Brennan, J. G. *Chem. Mater.* **2007**, *19*, 2937.
(9) (a) Kornienko, A.; Kumar, G. A.; Riman, R. E.; Emge, T. J.; Brennan, J. G. *J. Am. Chem. Soc.* **2005**, *127*, 3501. (b) Huebner, L.; Kornienko, A.; Emge, T. J.; Brennan, J. G. *Inorg. Chem.* **2005**, *44*, 5118.
(10) Banerjee, S.; Kumar, G. A.; Riman, R.; Emge, T. J.; Brennan, J. *J. Am. Chem. Soc.* **2007**, *129*, 5926.
(11) Romanelli, M. D.; Kumar, G. A.; Riman, R. E.; Emge, T. J.; Brennan, J. G. *Angew. Chem.* **2008**, *47*, 6049.
(12) Kornienko, A.; Banerjee, S.; Kumar, G. A.; Riman, R. E.; Emge, T. J.; Brennan, J. G. *J. Am. Chem. Soc.* **2005**, *127*, 14008.

Table 1. Summary of Crystallographic Details for **1** and **3**[a]

compound	**1**	**3**
Empirical formula	$C_{231}H_{215}N_{27}NaCe_{17}Se_{34}$	$C_{231}H_{215}N_{27}NaNd_{17}Se_{34}$
fw	8458.97	8529.01
space group	*C*2/*c*	*C*2/*c*
a (Å)	22.5455(11)	22.4939(13)
b (Å)	42.056(2)	41.963(2)
c (Å)	31.0886(16)	30.9247(17)
β (deg)	108.099(1)	108.129(1)
V (Å^3)	28019(2)	27741(3)
Z	4	4
D(calcd) (g/cm^{-3})	2.005	2.042
Temperature (K)	100(2)	100(2)
λ (Å)	0.71073	0.71073
abs coeff (mm^{-1})	7.165	7.629
independent reflns [$I > 2\sigma(I)$]	30853 [R(int) = 0.053]	28496 [R(int) = 0.049]
$R(F)$ [$I > 2\ \sigma(I)$][b]	0.0509	0.0516
$R_w(F^2)$ [$I > 2\ \sigma(I)$][c]	0.1426	0.1425

[a] Additional crystallographic details are given in the supporting information. [b] $R(F) = \sum||F_o| - |F_c||/\sum|F_o|$. [c] $R_w(F^2) = \{\sum[w(F_o^2 - F_c^2)^2]/\sum[w(F_o^2)^2]\}^{1/2}$.

2853 (s), 1576 (w), 1459 (m), 1376 (m), 1260 (m), 1091(m), 1020 (m), 799 (m), 700 (m) cm^{-1}.

X-ray Structure Determination. Data for **1**−**3** were collected on a Bruker Smart APEX CCD diffractometer with graphite monochromatized Mo Kα radiation (λ = 0.71073 Å) at 100K. Crystals were immersed in Paratone oil and examined at low temperatures. The data for **2** were used only to determine the unit cell parameters. The data for **1** and **3** were corrected for Lorenz effects and polarization, and absorption, the latter by a multiscan (SADABS)[13] method. The structures of **1** and **3** were solved by direct methods (SHELXS86).[14] All non-hydrogen atoms were refined (SHELXL97)[15] based upon F_{obs}^2. All hydrogen atom coordinates were calculated with idealized geometries (SHELXL97). Scattering factors (f_o, f', f'') are as described in SHELXL97. Crystallographic data and final R indices for **1** and **3** are given in Table 1. An ORTEP diagram[16] for the common structure of **1**, **2**, or **3** is shown in Figure 1. Complete crystallographic details are given in the Supporting Information.

LaF_3:Nd(0.5at%) Synthesis. LaF_3:Nd particles were synthesized using a hydrothermal process[17] and used as a basis of comparison for the emission properties of Nd clusters. Stoichiometric amounts of lanthanum(III) nitrate, neodymium(III) nitrate, and NH_4F (Sigma Aldrich, St. Louis, MO) were mixed in ∼75 mL of water for 30 min. This mixture was next transferred to a 125 mL Teflon linear and heated to ∼200 °C for 2 h in a Parr pressure vessel (Parr Instrument Company, Moline, IL). The as-synthesized nanoparticles were washed three times in deionized water by centrifuging and dried at 70 °C in an oven (Thermo Scientific Thermolyne, Waltham, MA) for further powder characterization. Heat-treatment of as-synthesized particles was completed in a controlled environment using the double crucible method[18] to prevent LaF_3 oxidation. Alumina crucibles (10 and 50 mL; CoorsTek, Golden, CO) were used for the heat treatment: ∼0.9 g of as-synthesized nanoparticles (inner 10 mL crucible) was heated with ∼3.0 g of 95% ammonium bifluoride (outer 50 mL crucible) at ∼400 °C for 1 h in a box furnace. The ionic concentration of Nd corresponding to 0.5 mol % is approximately 9×10^{19} ions/cc.

Spectroscopy. Absorption measurements were carried out in THF solution using an integrating sphere of a double beam spectrophotometer (Perkin-Elmer Lambda 9, Wellesley, MA). The emission spectra of a powdered sample were recorded by exciting the sample with a 0.7 W, 800 nm photodiode from BW Tec (Newark, NJ). The 900−1500 nm emission from the sample was focused onto a 0.55 m monochromator (Jobin Yvon, Triax 550, Edison, NJ) and detected by a thermoelectrically cooled InGaAs detector. The signal was intensified with a lock-in amplifier (SR 850 DSP, Stanford Research System, Sunnyvale, CA) and processed with a computer controlled by the Synerjy commercial software. To measure the decay time, the laser beam was modulated by a chopper and the signal was collected on a digital oscilloscope (TDS 220, 200 MHz, Tektronix, Beavetron, OR). The emission spectra from 1700−1900 nm excited at ∼800 nm with a 0.7 W laser (BW976, BW Tek, Newark, NJ) was collected using the FSP920 Edinburgh Instruments spectrometer (Edinburgh Instruments, Livingston, United Kingdom) that was equipped with a Hamamatsu G5852-23 thermoelectrically cooled shortwave infrared sensitive InGaAs photodiode. The emission data analysis follows our earlier work.[6−12]

Results and Discussion

Reactions of $Ln(SePh)_3$ (Ln = Ce (**1**), Pr (**2**), Nd (**3**)) with elemental Se in the presence of Na ions selectively precipitate the heptadecanuclear clusters $(py)_{16}Ln_{17}NaSe_{18}(SePh)_{16}$. In the absence of Na^+, the only products isolated from similar reactions are either $(py)_8Nd_8Se_6(SePh)_{12}$,[19] or polychalcogen species if the reaction mixtures contain large excesses of elemental Se.[20] These reactions depend on fractional crystallization for product isolation, and so the inclusion of Na within the cluster framework indicates only that the presence of a monovalent cation with this precise ionic radius leads to the formation of a relatively insoluble product. In contrast with the heterometallic chemistry of $Ln(ER)_3$ and $M(ER)_2$ (M = Zn, Cd, Hg),[21] where the presence of both metal types in solution always leads to a heterometallic product, the ionic alkali ions have only occasionally formed heterometallic products with Ln chalcogenolates[22] (i.e., $(py)_2YbLi(SePh)_4$ and $(THF)_2YbNa(TePh)_3$), and there is no clear chemical driving force behind the formation of Ln/alkali heterometallic products. The presence of Na ions simply offers additional flexibility in the process of forming insoluble products with surface ligands that are efficiently packed. This flexibility is specific, as the presence of Li or K led only to the isolation of previously reported $Nd_8Se_6(SePh)_{12}$. In considering

(13) Bruker-ASX. *SADABS, Bruker Nonius area detector scaling and absorption correction*, v2.05; Bruker-AXS Inc.: Madison, WI, 2003.
(14) Sheldrick, G. M. *SHELXS86, Program for the Solution of Crystal Structures*; University of Göttingen: Germany, 1986.
(15) (a) Sheldrick, G. M. *Acta Crystallogr.* **2008**, *A64*, 112. (b) Sheldrick, G. M. *SHELXL97, Program for Crystal Structure Refinement*; University of Göttingen: Germany, 1997.
(16) Graphics programs: ORTEP-3 for Windows: Farrugia, L. J. *J. Appl. Crystallogr.* **1997**, *30*, 565. Burnett, M. N.; Johnson, C. K. *ORTEP-III: Oak Ridge Thermal Ellipsoid Plot Program for Crystal Structure IllustrationsOak Ridge National Laboratory Report ORNL-6895*, 1996; Persistence of Vision Pty. Ltd., *Persistence of Vision Raytracer* (Version 3.6) 2004.
(17) (a) Wang, X.; Zhuang, J.; Peng, Q.; Li, Y. *Inorg. Chem.* **2006**, *45*, 6661. (b) Kumar, G. A.; Chen, C. W.; Ballato, J.; Riman, R. E. *Chem. Mater.* **2007**, *19*, 1523.
(18) Tan, M. C.; Kumar, G. A.; Riman, R. E. *Opt. Express* **2009**, *17*, 15904.
(19) (a) Melman, J. H.; Emge, T. J.; Brennan, J. G. *Chem. Commun.* **1997**, 2269. (b) Melman, J. H.; Emge, T. J.; Brennan, J. G. *Inorg. Chem.* **1999**, *38*, 2117. (c) Freedman, D.; Emge, T. J.; Brennan, J. G. *Inorg. Chem.* **1999**, *38*, 4400. (d) Freedman, D.; Emge, T. J.; Brennan, J. G. *J. Am. Chem. Soc.* **1997**, *119*, 11112.
(20) Kornienko, Anna, Y. Lanthanide and Heterometallic Chalcogenido Clusters. Ph.D Thesis, Rutgers, the State University of New Jersey, 2003.
(21) (a) Lee, J. S.; Emge, T. J.; Brennan, J. G. *Inorg. Chem.* **1997**, *36*, 5064. (b) Berardini, M.; Emge, T.; Brennan, J. *Inorg. Chem.* **1995**, *34*, 5327. (c) Berardini, M.; Emge, T.; Brennan, J. *J. Am. Chem. Soc.* **1994**, *116*, 6941. (d) Banerjee, S.; Sheckelton, J.; Emge, T. J.; Brennan, J. G. *Inorg. Chem.* **2010**, *49*, 1728. (e) Brewer, M.; Lee, J.; Brennan, J. G. *Inorg. Chem.* **1995**, *34*, 5919.
(22) (a) Berdardini, M.; Emge, T. J.; Brennan, J. G. *J. Chem. Soc. Chem. Commun.* **1993**, 1537. (b) Khasnis, D. V.; Brewer, M.; Lee, J. S.; Emge, T. J.; Brennan, J. G. *J. Am. Chem. Soc.* **1994**, *116*, 7129.

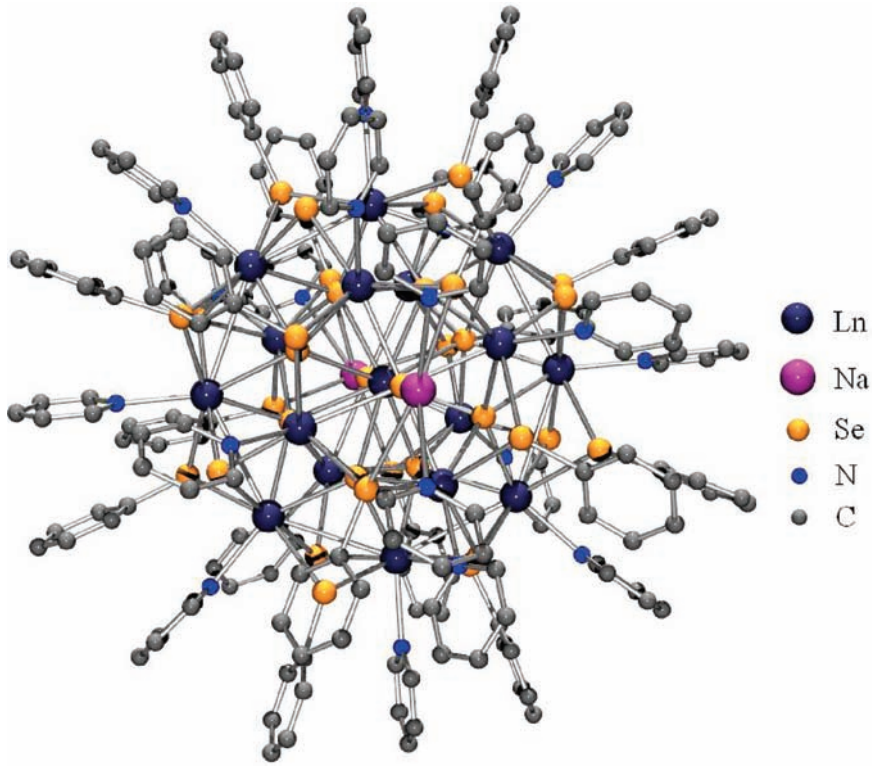

Figure 1. POV-Ray image of the ORTEP diagram of $(py)_{16}Ln_{17}NaSe_{18}(SePh)_{16}$, using spheres of arbitrary size. Both "capping" unique Na sites are shown (magenta), but only one is occupied for a given molecule.

the role of Na binding to nearby Se, selenolate, or py groups for the title compound, the cluster has two available sites on the surface for Na binding to Se which can also accommodate at least two more distant Na···py contacts to complete the Na coordination. For the instances where Na is absent, the site does not necessarily contain voids, and py molecules of solvation can apparently shift position slightly to adequately fill the site. Such shifts of py groups into and away from the generalized Na site occur with, but are not necessarily correlated to, the disorder of nearby selenolate ligands. Thus, the requirements of size and binding at the Na site are lax enough to accommodate either bound Na or free py molecules. It then appears reasonable that this "soft" binding requirement may disappear upon the use of other alkali that have quite different radii and electronic properties, and as a result, the partial occupancy requirement will also disappear and a different structure would ensue.

The presence of Na in cluster chemistry does not necessarily lead to significant changes in product identity. One of the first LnSe cluster reports in the literature described $Cp^*_6Sm_6Se_{11}$,[23] an octahedral arrangement of Cp*Sm connected by a mixture of Se and (SeSe) dianions. This was followed by the description of $(Cp'_6Sm_6Se_{13})Na(THF)_6$,[24] which contained the same octahedral arrangement of CpSm connected by a slightly different chalcogenido core, with a sodium ion that was totally uninvolved in bonding to the cluster. The difference between these organometallic systems and the present chalcogenolate compounds can be attributed to the overwhelming steric demands of substituted Cp ligands that tend to dictate structural features. This use of electronically inactive metal ions to dramatically alter the identity of a cluster product is an attractive new variable that can be manipulated to rationally deliver monodisperse clusters with a range of sizes.

Clusters **1**−**3** were characterized as isostructural by use of low temperature single crystal X-ray diffraction data. Individual structures were determined for **1** and **3**. Figure 1 shows an ORTEP diagram of the common cluster core for **1**−**3** (using data from **3**). The spherically shaped molecule of **3** is built upon a central Nd ion that resides on a crystallographic two-fold axis. This Nd is surrounded by 8 μ_5 selenido ligands that are further enveloped by a shell of 16 additional Nd ions, of which eight are seven-coordinate and eight are eight-coordinate. The coordination spheres of these outer Nd ions are then saturated an array of μ_3 and μ_5 Se^{2-}, μ_3 and μ_4 SePh, and pyridine ligands. The Na ion is also found on the surface of the cluster, bound on one side to an exposed selenido atom and two selenolate ligands (that bridge to Nd ions), and bound on its other side to pyridine ligands. Since there is one Na ion per cluster and two Na-containing sites per cluster and each site is on a crystallographic two-fold axis, the site occupancy of each unique Na atom is 25%. As expected, the two selenolates that bind to the Na are also two-fold disordered, each with one site having the phenyl group directed away from the Na site (i.e., when the Na is present) and one site having the phenyl group directed toward the Na site (i.e., when the Na is absent). The center of mass for either selenolate position is located at approximately the same place on the surface of the cluster, conserving size and shape requirements of the adjacent Nd ions. The pyridine molecules bonded to the Na ion appear to have considerable disorder, consistent with the fact that half the time they are occupying large cavities as lattice solvent molecules, that is, when the Na is absent.

There are remarkably few lanthanide clusters in the literature that contain internal, anion encapsulated Ln,[9,11] with most

(23) Evans, W. J.; Rabe, G. W.; Ansari, M. A.; Ziller, J. W. *Angew. Chem., Int. Ed. Engl.* **1994**, *33*, 2110.
(24) Jin, G.; Cheng, Y.; Lin, Y. *Organometallics* **1999**, *18*, 5735.

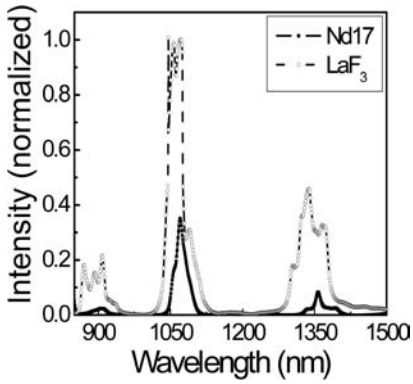

Figure 2. Emission spectrum of $(py)_{16}Nd_{17}NaSe_{18}(SePh)_{16}$ in comparison with Nd doped LaF_3.

compounds containing only surface Ln that coordinate solvent molecules or other ancillary ligands that might quench NIR emission. For example, even the largest reported Ln cluster, $[Gd_{54}Ni_{54}(ida)_{48}(OH)_{144}(CO_3)_6(H_2O)_{25}](NO_3)_{18}$, is built around a central Gd ion that coordinates a water molecule.[25] Of the few compounds that do have both internal and surface Ln, only **3** and the fluoride cluster $(py)_{24}Ln_{28}F_{63}(SePh)_{21}$ (Nd28) have a homogeneous set of core anions that can afford direct comparisons of chemical and physical properties with binary solid-state materials. In **3**, the central Nd is similar to the Nd ions in Nd_2Se_3[26] in that both contain eight coordinate ions. In Nd_2Se_3, there are two distinct sets of Nd−Se bond lengths (2.967 and 3.173) for the irregular LnA_4B_4 dodecahedron, whereas in **3**, the Nd−Se bond lengths are found in a narrow range (3.131−3.138 Å, avg. 3.135 Å). Although the cluster and solid state Nd environments are similar, the Se geometries differ. Each Se in Nd_2Se_3 is in octahedral or near-octahedral sites, that is, coordination numbers of either five or six in a 2:1 ratio. In contrast, all the selenido ligands bound to the central Nd ion, that is, the "core" of the cluster, coordinate to five Nd, with Nd−Se−Nd angles that are severely distorted from any idealized geometry.

The potential utility of the cluster as a signal amplification source in polymer optical fibers mandates an evaluation of their emission properties. The absorption spectrum of **3**, given in the Supporting Information, is similar to Nd^{3+} spectral transitions of typical solid-state materials with comparable absorbance.[27] Judd-Ofelt parameters[28,29] were subsequently extracted from the absorption spectrum to calculate radiative lifetime (τ_{rad}). The emission spectrum, obtained by exciting the metastable level $^4F_{3/2}$, with 800 nm light, is shown in Figures 2 and 3. A cascade of well resolved emission bands are observed at 907, 1070, 1357, and 1822 nm corresponding to the $^4F_{3/2} \rightarrow {}^4I_{9/2}$, $^4F_{3/2} \rightarrow {}^4I_{11/2}$, $^4F_{3/2} \rightarrow {}^4I_{13/2}$, and $^4F_{3/2} \rightarrow {}^4I_{15/2}$ transitions, respectively. Even though emission wavelengths from a variety of Nd-based materials are consistent from one host to another due to the strong outer $5s^25p^6$ orbital shielding, the emission intensity and efficiency vary dramatically.

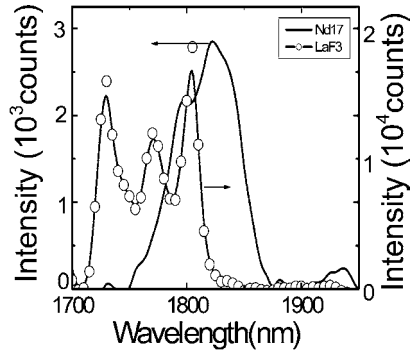

Figure 3. Low energy emission spectrum of $(py)_{16}Nd_{17}NaSe_{18}(SePh)_{16}$ in comparison with Nd doped LaF_3.

To measure the quantum efficiency of the $^4F_{3/2} \rightarrow {}^4I_{11/2}$ transition (1070 nm emission), the fluorescence decay time (τ_{fl}) was extracted from the measured decay curve. The decay curve was fitted with the Monte Carlo model[30] to yield a decay time of 330 μs for the 1070 nm emission. The fitting takes into account all the cooperative energy transfer and cross-relaxation processes between Nd atoms located in the various crystallographic sites. The experimental decay time, together with the calculated radiative decay time,[28,29] results in a calculated quantum efficiency of 35% for **3**.

The quantum efficiency reflects the extent to which nonradiative processes dominate the relaxation from a selected excited state. The smaller the energy gap between the emissive state and highest sublevel of its ground or receiving multiplet, the easier it is for the gap to be closed by nonradiative relaxation processes (e.g., through presence of high phonon energy bonds, C−H, N−H or O−H). The fluorescence lifetimes of lanthanide materials depend mainly on the lattice properties of the host, in terms of both lattice vibrations and internuclear Ln−Ln distances, and cluster **3** allows us to outline how quantum efficiency depends upon lattice. When compared with the efficiency of 9% found for $(DME)_2Nd(SC_6F_5)_3$, 16% in $(THF)_8Nd_8O_2Se_2(SePh)_{14}$ ("Nd8"),[8b] and 12% in $(py)_{18}Nd_{12}O_6Se_{12}(SePh)_8(SeSePh)_2Hg^+$ (Nd12), the 35% value found for **3** clearly illustrates that increasingly large molecules display increasingly bright photophysical properties. A correlation of brightness with cluster size is understandable, given that as the size of the emission source increases, the ratio of [emission quenching functional groups]/Nd decreases, with the ultimate limit being the 100% efficiencies found in bulk solid-state Nd doped sulfide materials.[31] In Nd compounds, the $^4F_{3/2} \rightarrow {}^4I_{11/2}$ transition (1070 nm emission) is quenched by the third order vibrational overtone of CH bonds. The number of CH bonds found in the ligands (THF, py, SePh) directly bound to the cluster surfaces are 136 (Nd8), 140 (Nd12), 167 (**3**), and 225 (Nd28). Thus, on an average per Nd ion, the number of CH in Nd8 is 17, in Nd12 is 12, in **3** is 10, and in Nd28 is 8. Considering this, the nonradiative losses from the surrounding CH groups are least in the larger clusters, and this accounts for the lower efficiency of the fluoride cluster relative to **3**, when both solid state Nd: La_2S_3[31] and Nd:LaF_3[32] have 100% quantum efficiencies.

(25) Kong, X.; Ren, Y.; Chen, W.; Long, L.; Zheng, Z.; Huang, R.; Zheng, L. *Angew. Chemie, Int. Ed.* **2008**, *47*, 2398.
(26) Schneck, C.; Hoess, P.; Schleid, T. *Acta Crystallogr., Sect. E* **2009**, *E65*, i20/1.
(27) (a) Oczko, G. *J. Alloys Comp.* **2000**, *300*, 414. (b) Lis, S. *J. Alloys Comp.* **2000**, *300*, 88. (c) Gubina, K. E.; Shatrava, J. A.; Ovchynnikov, V. A.; Amirkhnov, V. M. *Polyhedron* **2000**, *19*, 2203. (d) Legendziewicz, J.; Oczko, G.; Wiglusz, R.; Amirkhanov, V. *J. Alloys Comp.* **2001**, *323*, 792.
(28) Judd, B. R. *Phys. Rev B.* **1962**, *127*, 750.
(29) Ofelt, G. S. *J. Chem. Phys.* **1962**, *37*, 511.
(30) Díaz Torres, L. A.; Barbosa-Garcia, O.; Meneses-Nava, M. A.; Struck, C. W.; Di Bartolo, B. In *Advances in Energy Transfer Processes*; Di Bartolo, B., Chen, X., Eds.; World Scientific Publishing Co.: Singapore, 2000; pp 523−552.
(31) (a) Schweizer, T. Ph.D. Thesis, Universitat Hamburg, 1998. (b) *Optical Fiber Amplifiers—Materials, Devices, and Applications*; Sudo, S., Ed; Artech House Inc.: Norwood, MA, 1997.

Comparative emission efficiencies are also affected by lattice compositions. Anions that have low phonon characteristics lead to particularly emissive materials. Of the anions discussed here, oxide ligands generate high-phonon energy lattices, while the heavier chalcogenide and low force constant fluoride anions provide low-phonon environments. In Nd8, there are 50 Nd−Se and six Nd−O^{2-} bonds; in Nd12 there are 56 Nd−Se bonds and 24 Nd−O^{2-} bonds, in **3** there are 107 Nd−Se bonds, and in Nd28, there are 192 Nd−F bonds and 36 NdSe bonds. Even though detailed energy transfer calculations have not yet been carried out in **3** to understand the impact of Nd atomic distribution on the luminescence efficiency, it is clear that **3** is brighter than the oxide containing clusters because of the higher energy associated with the Nd−O bond,[7c] and is comparable with the fluoride cluster because all anions have low phonon characteristics.

These comparative emission efficiencies are also impacted by lattice dependent Nd−Nd separations. The shortest Nd−Nd separations for Nd8, Nd12, **3**, and Nd28 are 3.82, 3.77, 3.75, and 3.89, respectively, with the greatest separations coming in the cluster with the smallest anion (that leads to higher coordination numbers, and thus greater effective ionic radii, for Ln). These distances are crucial to the inhibition of energy migration processes that reduce the intensity of the 904 and 1070 nm emissions,[30] and again help to account for the slightly greater emission efficiency of the fluoride cluster.

The emission spectrum of **3** is also interesting in that the $^4F_{3/2} \rightarrow {}^4I_{15/2}$ transition is also observed at room temperature. This relatively low energy (1.8 μm) transition is extremely unusual, and was not noted in either the $Nd_{12}O_6$ or the $Nd_{28}F_{63}$ fluoride clusters. This transition has been observed in solid-state chalcogenides,[31] fluorides,[32,33] and tellurite glasses,[34] all of which are considered low phonon host environments, although curiously this emission has not been observed from NdF_3. Similarly, in molecular systems, this transition has also been observed in Nd8[8b] and $(DME)_2Nd(SC_6F_5)_3$ (but not in the spectrum of $Nd(OC_6F_5)_3$[6] or Nd12[10]). An analysis of the quenching pathways in the larger oxo compound suggested that the loss of this low energy relaxation pathway was the result of multiphonon relaxation, and the emission noted here is again consistent with the phonon characteristics of the selenido lattice.

Conclusion

Spectroscopically silent metal ions can be used to generate increasingly large lanthanide clusters. The Nd cluster $(py)_{16}Nd_{17}NaSe_{18}(SePh)_{16}$ is a particularly bright NIR emission source because it combines a high concentration of Nd encapsulated by a low-phonon environment and relatively few C−H bonds close to Nd.

Acknowledgment. J.G.B. acknowledges the support of NSF (CHE-0747165) and R.E.R. acknowledges support from the Defense Advanced Research Project Agency (ONR N00014-08-1-0131).

Supporting Information Available: Fully labeled ORTEP diagrams and X-ray crystallographic files in CIF format for the crystal structures of **1** and **3**. Absorption spectrum for **1**−**3** and fluorescence decay for **3**. This material is available free of charge via the Internet at http://pubs.acs.org.

JA1069322

(32) (a) Kumar, G. A.; Chen, C. W.; Riman, R. E. *Chem. Mater.* **2007**, *19*, 1523. (b) Tan, M. C.; Kumar, G. A.; Riman, R. E.; Brik, M. G.; Hommerich, U. *J. Appl. Phys.* **2009**, *106*, 063118.

(33) (a) Davey, S. T.; France, P. W. *Br. Telecom. Tech. J.* **1988**, *7*, 58. (b) Stouwdam, J. W; van Veggel, F. C. J. M. V. *NanoLett.* **2002**, *2*, 733. (c) Shen, S.; Jha, A.; Zhang, E.; Wilson, S. J. *C. R. Chim.* **2002**, *5*, 921. (d) Payne, S. A.; Bibeau, C. *J. Lumin.* **1998**, *79*, 143.

(34) Shen, S.; Jha, A.; Zhang, E.; Wilson, S. J. *C. R. Chim.* **2002**, *5*, 921.